



Since January 2020 Elsevier has created a COVID-19 resource centre with free information in English and Mandarin on the novel coronavirus COVID-19. The COVID-19 resource centre is hosted on Elsevier Connect, the company's public news and information website.

Elsevier hereby grants permission to make all its COVID-19-related research that is available on the COVID-19 resource centre - including this research content - immediately available in PubMed Central and other publicly funded repositories, such as the WHO COVID database with rights for unrestricted research re-use and analyses in any form or by any means with acknowledgement of the original source. These permissions are granted for free by Elsevier for as long as the COVID-19 resource centre remains active.

Epimedium-derived phytoestrogen exert beneficial effect on preventing steroid-associated osteonecrosis in rabbits with inhibition of both thrombosis and lipid-deposition

G. Zhang^a, L. Qin^{a,*}, H. Sheng^a, K.W. Yeung^b, H.Y. Yeung^a, W.H. Cheung^a, J. Griffith^b, C.W. Chan^c, K.M. Lee^c, K.S. Leung^a

^a Musculoskeletal Research Laboratory, Department of Orthopaedics and Traumatology, The Chinese University of Hong Kong, Shatin, N.T., Hong Kong SAR, PR China

^b Department of Organ and Imaging, The Chinese University of Hong Kong, Hong Kong SAR, PR China

^c Lee Hysan Clinical Laboratory, The Chinese University of Hong Kong, Hong Kong SAR, PR China

Received 15 August 2006; revised 14 October 2006; accepted 25 October 2006
Available online 22 December 2006

Abstract

Objectives: This study tested the effect of Epimedium-derived phytoestrogen (PE) on preventing steroid-associated osteonecrosis (ON) in rabbit model.

Methods: Thirty 28-week-old male New-Zealand white rabbits were divided into control group (CON; $n=14$) and PE group (PE; $n=16$; 5 mg/kg body weight/day) after receiving an established inductive protocol for inducing steroid-associated ON. Before and after inductive protocol, Dynamic-MRI was employed on bilateral femora for local intra-osseous perfusion, blood samples were examined for coagulation, fibrinolysis and lipid-transportation, and marrow samples were quantified for adipogenesis-gene mRNA expression. Six weeks later, bilateral femora were dissected for Micro-CT-based micro-angiography, and then ON lesion, intravascular thrombosis and extravascular fat-cell-size were examined histopathologically.

Results: The incidence of ON in the PE group (31%) was significantly lower than that in the CON group (93%). Compared to the CON group, local intra-osseous perfusion was maintained in the PE group. Blocked trunk vessels were seldom found in micro-angiography of the PE-treated rabbits. Thrombosis incidence and fat-cell-size were both significantly lower in the PE group than those in the CON group. During the early period after induction, indicator of coagulation, fibrinolysis, lipid-transportation and adipogenesis-gene expression were found with significantly changing pattern in the PE group compared to the CON group.

Conclusion: PE was able to exert beneficial effect on preventing steroid-associated ON in rabbits with inhibition of both thrombosis and lipid deposition.

© 2006 Elsevier Inc. All rights reserved.

Keywords: Steroid-associated osteonecrosis; Epimedium-derived phytoestrogen; Intravascular thrombus occlusion; Extravascular lipid deposition; Blood perfusion; Ischemia

Introduction

Steroid is commonly prescribed for treatment of medical conditions. Inevitably, steroid-associated osteonecrosis (ON) is frequently reported [1–3], which has been recently highlighted after life-saving treatment for Severe Acute Respiratory Syndrome (SARS) patients [4–6]. Total joint replacement

(TJR) is the last option for treatment of ON, yet the post-surgical prognosis is poor in ON patients treated with steroid [7]. Therefore, prevention of development of steroid-associated ON before formation of ON lesions is highly desirable [2,3].

A consensus etiopathogenesis of steroid-associated ON has been recently unified on both intravascular thrombosis-induced occlusion and extravascular lipid-deposit-induced compression, leading to an impaired structure–function of intra-osseous blood supply system [2,3,8,9]. For intravascular thrombosis, imbalance between coagulation and fibrinolysis, which predisposes

* Corresponding author. Fax: +852 26324618.

E-mail address: Lingqin@cuhk.edu.hk (L. Qin).

to both hypercoagulation and hypofibrinolysis, has consistently presented itself in the intravascular events [10,11,14]. For extravascular lipid deposition, abnormal lipid transportation to the peripheral tissue [12] and excessive PPAR γ 2-mediated adipogenesis [13] has been involved in extravascular events. Although it has been experimentally confirmed that a combined administration of an anticoagulant with a lipid-lowering agent may help prevent steroid-associated ON in rabbits [15], an ideal strategy is highly desirable to simultaneously target both intravascular thrombosis and extravascular lipid deposition for preventing steroid-associated ON [3].

Outbreak of SARS in China in 2003 provides a unique opportunity of evidence-based medicine for studying steroid-associated ON. There is a remarkable difference in prevalence of ON recovered from SARS patients between North China 32.7% [6] and South China 5–6% [4,5]. Interestingly, the frequency of herb preparation used for SARS patients during rehabilitation after pulsed steroid-treatment was much higher in South China (conventional herbal intervention with WHO recommended procedure) than in North China (WHO recommended procedure without conventional herbal intervention) [16–18]. The lower ON prevalence in South China was suggested to be associated with their potential effects on prevention of steroid-associated ON. Antiviral herbal *Epimedium* with immunomodulation was one of the medicinal herbs [17], which has been also used as a broad-spectrum ‘bone strengthening’ herb in traditional Chinese medicine to treat many musculoskeletal diseases [19].

To date, a group of phytoestrogen fractions has been derived from *Epimedium* (PE) by a series of standardized isolation procedures, which consists of three bioactive phytoestrogenic compounds (Icariin, Genistein and Daidzein) [19–21] (Fig. 1). This phytoestrogen-rich PE, has been proven to be safe and become an alternative preparation for long-term administration without reported notable side effects to prevent postmenopausal osteoporosis [19,22,23]. In terms of potential extravascular efficacy, phytoestrogen (either Genistein or Daidzein) has been shown to be able to decrease low-density lipoprotein, increase high-density lipoprotein [24–26] and downregulate PPAR γ 2 gene expression [27–30]. This implies a potential capability of inhibiting extravascular lipid deposition in peripheral tissues. In terms of potential intravascular efficacy, phytoestrogen (either

Icariin or Daidzein) has been reported with potential anti-thrombotic activities intravascularly through a mechanism of maintaining balance between coagulation and fibrinolysis [31,32,40]. However, the prevention effect of PE on steroid-associated ON has not been studied scientifically. Accordingly, we hypothesized that PE might exert beneficial effect on preventing steroid-associated ON development with inhibition of both thrombosis and lipid deposition. A recently established steroid-associated ON rabbit model with high incidence of ON and no mortality of animals was used to test the hypothesis [9].

Materials and methods

Animal, grouping and treatment

Thirty male 28-week-old New-Zealand white rabbits with body weight of 4–5 kg were housed at the Experimental Animal Center of Prince of Wales Hospital, and received a standard laboratory diet and water *ad libitum*. The experimental protocol was approved by the Animal Experiment Ethics Committee of The Chinese University of Hong Kong (Ref No. 04/038/MIS). Based on our established protocol for inducing steroid-associated ON [9], all the rabbits were intravenously injected with 10 μ g/kg body weight of Lippolysaccharide (LPS; *Escherichia coli* 0111:B4, Sigma-Aldrich, Inc. USA) on day 0 (week 0). 24 h later, three injections of 20 mg/kg body weight of Methylprednisolone (MPS; Pharmacia and Upjohn, USA) were given intramuscularly at a time interval of 24 h. They were then divided into control group (CON; $n=14$) with oral vehicle and PE group (PE; $n=16$, 5 mg/kg body weight/day) with oral PE for 6 weeks, beginning on day 0 before LPS injection. A specifically custom-made tube was used for oral administration [23]. Six weeks after LPS injection, all the rabbits were then euthanized for evaluations. Both control vehicle and PE (10 mg flavonoids preparation containing 5000 μ g Icariin, 250 μ g Genistein, 1250 μ g Daidzein and 3500 μ g vehicle) (Fig. 1) was commercially available (Tong Ji Tang Pharmacal Company, Gui Zhou, China). The time-point of 6 weeks for euthanasia was experimentally confirmed to present ON lesions accompanied by repair process in our most recent study which is equivalent to Stage II ON (Ficart and Arlet classification system) [9]. The body weight of the animals was recorded weekly for adjusting administration of PE. The final body weight before sacrifice was documented. Accident mortality in both groups was recorded throughout the experiment period.

Pre-euthanasia evaluation

Haematological examination for etiology

5 ml blood sample was collected immediately before injection of LPS, and at week 1, 2, 4 and 6 after LPS injection. Using our previously established protocol, plasma was prepared. Then, a half of the plasma was used for evaluating intravascular thrombotic status, including intravascular fibrinolysis

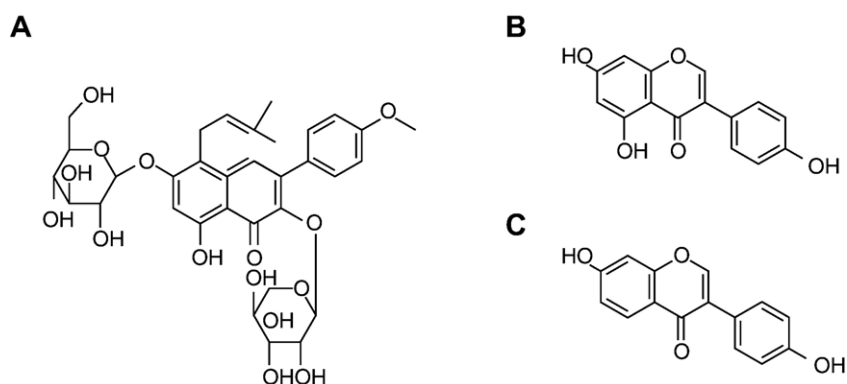


Fig. 1. Three bioactive phytoestrogenic compounds in *Epimedium*-derived flavonoids fractions. A: Icariin (50%); B: Genistein (2.5%); C: Daidzein (12.5%).

indicator *t-PA/PAI-I* (ratio of tissue-type-plasminogen-activator to plasminogen-activator-inhibitor) and intravascular coagulation indicator APTT (activated-partial-thromboplastin-time). Another half was for evaluating extravascular lipid deposition on aspect of lipid transport, i.e., *LDL/HDL* (ratio of low-density-lipoprotein-cholesterol to high-density-lipoprotein-cholesterol) [9].

Marrow RT-PCR analysis for etiology

For evaluating extravascular lipid deposition on aspect of adipogenesis, RT-PCR (Reverse transcription polymerase chain reaction) analysis was employed for determining *PPAR γ 2* (Peroxisome Proliferator-Activated Receptor-gamma2) mRNA expression (a key transcription factor responsible for adipocyte differentiation) of bone marrow mononuclear cells immediately before injection of LPS, at week 1, 2, 4 and 6 after LPS injection, using established protocol with GAPDH as internal control [22,27,33].

Dynamic-MRI for pathophysiology

Dynamic MRI for bilateral proximal or distal femur bilaterally was obtained before LPS injection, and at week 1, 2, 4 and 6 after LPS injection using a 1.5 T superconducting system (ACS-NT Intera; Philips, The Netherlands). Rabbits were anesthetized and placed in supine with the lower limb flexed and fixed by adhesive tape. An extremity coil (transmit-receive surface coil) was used on the target site. Preliminary sagittal and oblique axial images were obtained to define the local longitudinal axis. T1-weighted sequence (T1W, repetition time [TR]/echo time [TE]=425/13 ms) was employed in turn for the conventional MRI images of the target site [9]. Imaging parameters were as follows: section thickness of 3 mm, intersection gap of 1 mm, field of view of 120 mm and imaging matrix of 256×128. A receive-only surface coil was used to cover the target site. The contrast-enhanced dynamic MR pulse sequence used previously established ultrafast T1-weighted gradient-echo sequences (turbo-field echo; Philips) with TR=2.2 ms, TE=0.92 ms, pre-pulse inversion time=400 ms, flip angle=15°, scan percentage=40%, and acquisition matrix=128×128 [9]. A total of 200 dynamic images were obtained in 90 s. A bolus of dimeglumin gadopentetate (Magnevist; Schering, Berlin, Germany) (0.8 mmol/kg/body weight) was rapidly administered manually via a previously placed 21-gauge intravenous catheter in the right ear vein, immediately followed by a 6 ml saline flush at the same injection rate. The dynamic scan started as soon as the injection of the contrast medium commenced. Signal intensity (SI) was then measured in operator-defined ellipse-like regions of interest (ROIs) over

the target site beneath the joint space in the mid-coronal T1-weighted images using a cursor and graphic display device. The signal intensity values derived from the ROIs were plotted against time as time-intensity curve (TIC) using the Gyroview software system (Philips). The baseline value (SI_{base}) of the SI in a TIC was calculated as the mean SI value in the first three images. The maximum SI (SI_{max}) was defined as the peak enhancement value at a given time interval of 90 s after contrast injection during early phase of the first pass of contrast. Perfusion parameter was calculated namely: 'Maximum enhancement'. 'Maximum enhancement' was defined as the maximum percentage increase (SI_{max} - SI_{base}) in SI from baseline (SI_{base}) [34]. The perfusion parameter was calculated according to the following equation:

$$\text{Maximum enhancement} = \frac{(\text{SI}_{\text{max}} - \text{SI}_{\text{base}})}{\text{SI}_{\text{base}}} \times 100\%$$

Post-euthanasia evaluation

Perfusion and decalcification

Under general and deep anesthesia with Sodium Pentobarbital, the abdomen cavity of the animals was opened for perfusion with a conformed radiopaque silicone rubber [35] using our previously established protocol [9,36]. After that, bilateral femoral samples were decalcified completely for the following evaluations.

Micro-angiography for pathophysiology

Proximal or distal part of bilateral femoral samples from each rabbit was taken for MicroCT-based micro-angiography and quantified for *Connect Density* of angiographic structure using our previously established protocol [9]. In brief, both proximal or distal part of the bilateral femoral samples of each rabbit were placed with proximal or distal end into a Polymethylmethacrylat (PMMA) sample tube, respectively. The femoral shaft was fixed in the tube with its long axis perpendicular to the bottom of the tube for micro-CT scanning using μ CT-40 (Scanco Medical, Bassersdorf, Switzerland). The scan was then perpendicular to the shaft and initiated from a reference line 10 mm away from the bottom with an entire scan length of 10mm. The scan was preformed at a resolution of 36 μ m per voxel with 1024×1024 pixel image matrix. For segmentation of blood vessels from background, noise was removed using a low pass Gaussian filter (Sigma=1.2, Support=2) and blood vessels was then defined at a threshold of 85.

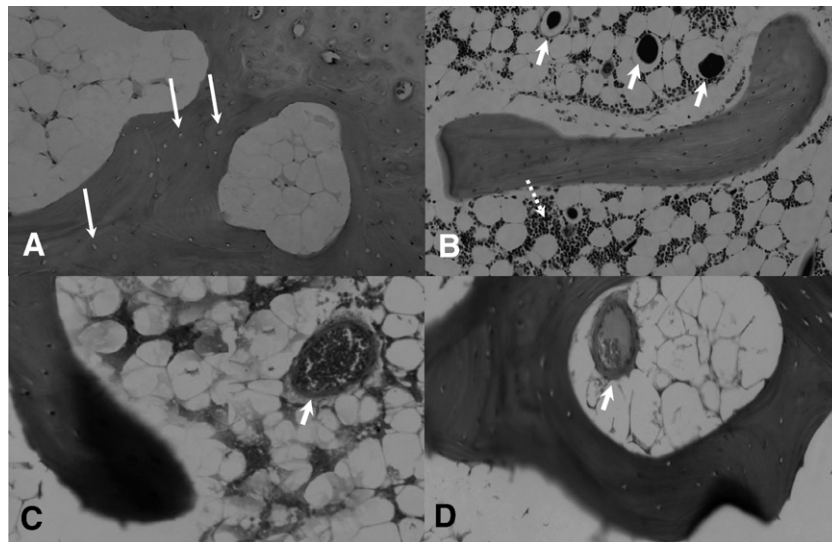


Fig. 2. Histopathological comparisons between ON⁺ sample in the CON group and ON⁻ sample in the PE group. A: Representative ON⁺ sample in the CON group showed more empty lacunae (indicated by arrow), which were surrounded by more marrow fat cells with increased size dominantly occupying marrow space (H&E, ×40). B: Representative ON⁻ sample in the PE group showed living bone with more osteocytes. Marrow space was preserved for marrow hematopoietic cells (indicated by dotted arrow) and vessels containing radiopaque substance (Microfil) indicated by arrow (H&E, ×40). C: No thrombus except erythrocyte (indicated by arrow) was found in vessel of representative ON⁻ sample in the PE group (H&E, ×80). D: Partial occlusion due to thrombosis (indicated by arrow) was found in vessel of representative ON⁺ sample in the CON group (H&E, ×80).

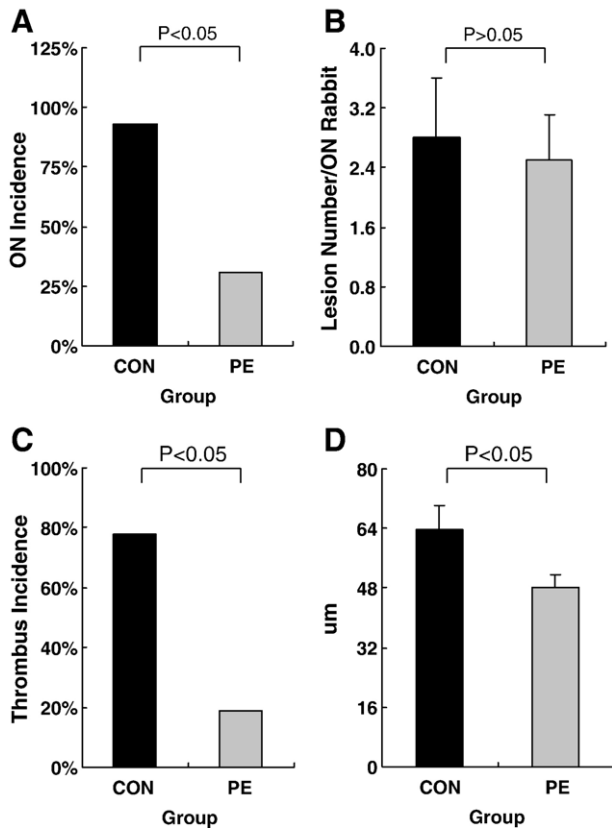


Fig. 3. Histological data compared between the PE group and the CON group. A: A lower ON incidence was found in the PE group (5/16) than the CON group (13/14) ($P<0.05$). B: No difference was found in number of lesions per ON⁺ rabbit between the CON group and the PE group ($P>0.05$). C: A lower thrombus incidence was found in the PE group (3/16) than the CON group (11/14) ($P<0.05$). D: The size of fat cells was found significantly lower in the PE group ($n=16$) than the CON group ($n=14$) ($P<0.05$).

Histopathology

Evaluation of ON lesions was performed using well established criteria [9,37,38]. Rabbit that had at least one osteonecrotic lesion in the areas examined was considered as ON⁺, while that with no osteonecrotic lesions were considered as ON⁻. The incidence of ON was defined as the numbers of ON⁺ rabbits divided by the numbers of total rabbits in each group. The extent of ON was defined as the numbers of ON lesions per affected rabbit.

Examination of intravascular thrombus and calculation of extravascular fat cell size were performed using our recently established protocol [9]. Rabbit that had at least one thrombotic lesion (Phosphotungstic Acid Hematoxylin Staining [9]) in the areas examined was considered as TH⁺, while that with no thrombotic lesions were considered as TH⁻. The incidence of thrombus was defined as the numbers of TH⁺ rabbits divided by the numbers of total rabbits in each group.

Statistics

Fisher's exact probability test was performed to determine the difference in incidence data ('ON Incidence' and 'Thrombus Incidence') between the CON group and the PE group. The cross-sectional comparison of 'Fat Cell Size', 'ON Extent' and '3-D Connect Density' between the CON group and the PE group was performed using Analysis of Covariance (ANCOVA) with body weight as covariant variable for eliminating its influence on the measurement results, especially for lipid metabolism data ('Fat Cell Size'). The longitudinal quantification data from hematological examination, RT-PCR analysis and Dynamic-MRI assessment were analyzed by 'ANOVA of Repeated Measures' with body weight as a covariant variable for eliminating its influence on the measurement results, especially for lipid metabolism data ('LDL/HDL'). All statistical analysis was performed using SPSS 10.0. Statistical significance for comparison was set at $P<0.05$.

Results

End-point evaluations for safety and efficacy

No rabbits died in both groups throughout the experimental period. The incidence of ON in the PE group was 31% (5/16), which was lower than 93% (13/14) in the CON group ($P<0.05$). There was no significant difference found in the extent of ON between the PE group (2.5 ± 0.6) and the CON group (2.8 ± 0.8) ($P>0.05$). ON lesions with typical features presented in all the ON⁺ rabbits (Figs. 2 and 3).

Intravascular/extravascular etiopathogenic events

Extravascular indicators

Histopathologically, the marrow fat cell size in the PE group was $48.17\pm 3.54\ \mu\text{m}$, which was significantly smaller than $63.71\pm 6.41\ \mu\text{m}$ of the CON group ($P<0.05$). In the PE group, marrow space

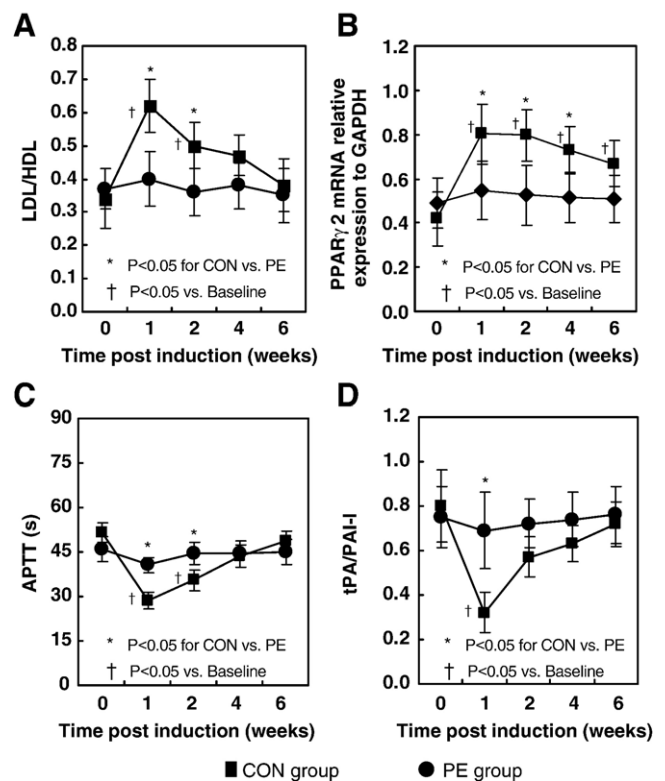


Fig. 4. Haematological and molecular data showed significantly different changing pattern over time between the CON group and the PE group ($P<0.05$). A: The LDL/HDL ratio showed a significant increase from baseline in the CON group at week 1 after LPS injection and declined towards baseline thereafter, whereas no significant increase was shown in the PE group after LPS injection ($P<0.05$). B: The marrow PPAR γ 2 mRNA relative expression level to GAPDH showed a significant increase from baseline ($P<0.05$) in the CON group at week 1 after LPS injection, then plateaued from week 1 to week 2 after LPS injection and declined towards baseline thereafter. With different pattern, no significant increase was shown in the PE group than after LPS injection. C: The APTT in the CON group presented a significant decrease from baseline at week 1 after LPS injection and returned to the baseline level thereafter, whereas no significant decrease was revealed in the PE group after LPS injection. D: The tPA/PAI-I ratio in the CON group significantly declined from baseline at week 1 after LPS injection and returned to the baseline thereafter, whereas no significant decrease was shown in the PE group after LPS injection ($P<0.05$).

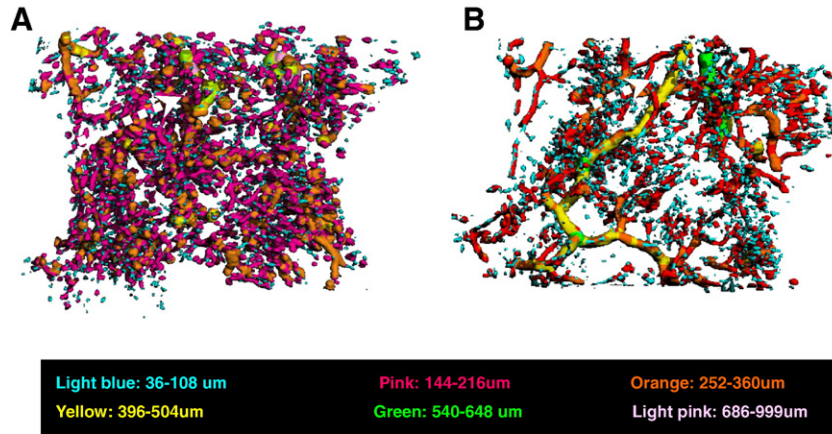


Fig. 5. Representative images of Micro-CT-based intraosseous micro-angiography of proximal femur. A: The ON⁺ proximal femur in the CON group showed a blocked trunk vessel with large diameter (marked with yellow) surrounded by numerous small disconnected vessels and disseminated leakage substance (Microfil). B: Neither blocked trunk vessels with large diameter (marked with yellow) nor numerous small disconnected vessels or disseminated leakage substance (Microfil) was shown in the ON⁻ proximal femur of the PE group. (For interpretation of the references to colour in this figure legend, the reader is referred to the web version of this article.)

was preserved for hematopoietic cells and vessels in ON⁻ rabbits. However, little space was left for marrow elements due to enlarged fat cell size in the ON⁺ rabbits (Figs. 2 and 3).

For lipid transportation, the LDL/HDL ratio showed a significant increase from baseline in the CON group at week 1 after LPS injection and declined towards baseline thereafter ($P < 0.05$), whereas no significant increase from baseline was shown in the PE group after induction (Fig. 4A).

For adipogenesis, the marrow PPAR γ 2 mRNA relative expression level showed a significant increase from baseline ($P < 0.05$) in the CON group at week 1 after LPS injection, then plateaued from week 1 to week 2 after LPS injection and declined towards baseline thereafter. In different pattern, no significant increase from baseline was shown in the PE group after induction (Fig. 4B).

Intravascular indicators

Histopathologically, thrombi were found in small marrow arteries around necrotic bone in ON⁺ rabbits. The incidence of

thrombus in the PE group was 19% (3/16), which was lower than 78% (11/14) in the CON group ($P < 0.05$) (Fig. 3).

For coagulation, the APTT in the CON group presented a significant decrease from baseline at week 1 after LPS injection and returned to the baseline level thereafter, whereas no significant decrease from baseline was revealed in the PE group after induction (Fig. 4C).

For fibrinolysis, the tPA/PAI-I ratio in the CON group significantly declined from baseline at week 1 after LPS injection and returned to the baseline thereafter, whereas no significant decrease from baseline was shown in the PE group after induction (Fig. 4D).

Pathophysiologic pathway for intra-osseous blood supply

Micro-CT based vascular network

The ON⁺ samples in the CON group showed blocked trunk vessels with large diameter, which were surrounded by both numerous small disconnected vessels and disseminated leakage

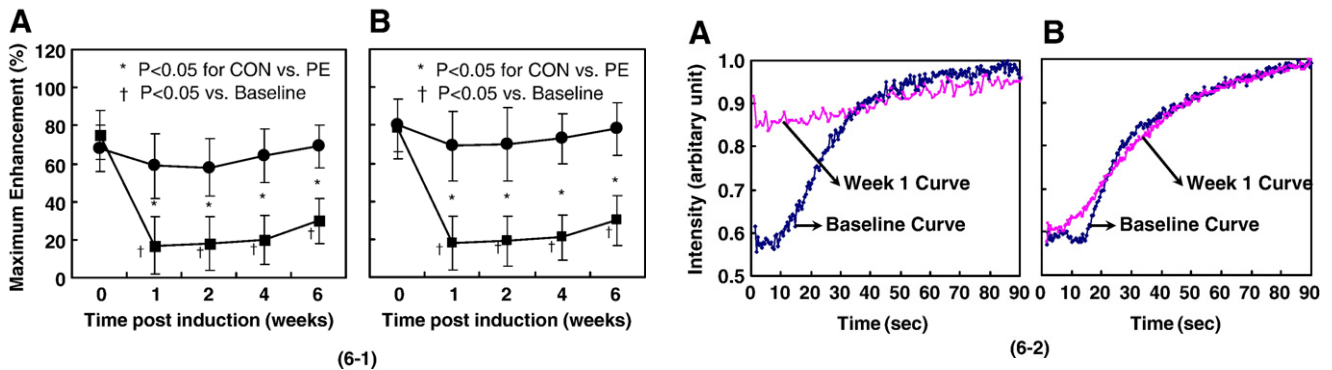


Fig. 6. (6-1) Blood perfusion assessed by dynamic MRI with significant difference in changes of curve pattern over time between the CON group and the PE group ($P < 0.05$). Maximum Enhancement at the examined sites (both proximal femur for A and distal femur for B) showed a significant decrease from baseline ($P < 0.05$) in the CON group at week 1 after LPS injection, then plateaued from week 1 to week 2 after LPS injection and increased moderately thereafter. With different patterns, no significant decrease was revealed in the PE group after LPS injection. (6-2) Representative Time-Intensity Curves derived from contrast-enhanced dynamic MRI on proximal femur. A: Maximum Enhancement showed a significant decrease from baseline in the CON group at week 1 after LPS injection. B: No significant decrease was found from the baseline in the PE group at week 1 after LPS injection.

substance (Microfil). In different pattern, there were neither blocked trunk vessels nor many small disconnected structural units in the ON⁻ samples from PE group (Fig. 5). 3-D Connect Density showed significantly lower in CON group (0.028 ± 0.014 , $1/\text{mm}^3$) than PE group (0.065 ± 0.006 , $1/\text{mm}^3$) ($P < 0.05$).

Dynamic MRI based perfusion function

A low signal area on T1-weighted MR image presented initially in ON⁺ rabbits of CON group at 2 weeks, whereas no suspicious signal area was found in ON⁻ rabbits of PE group throughout the experimental period. ‘Maximum Enhancement’ at the examined sites (both proximal and distal femur) showed a significant decrease from baseline ($P < 0.05$) in the CON group at week 1 after LPS injection, then plateaued from week 1 to week 2 after LPS injection and increased moderately thereafter. In different pattern, no significant decrease from baseline was revealed in the PE group after LPS injection (Fig. 6).

Discussion

The present study was the first one that demonstrated beneficial effect of a group of phytoestrogenic fractions derived from *Epimedium* (PE) in prevention of steroid-associated ON with inhibition of both thrombosis and lipid deposition in rabbit model.

A potential effective measure for prevention of steroid-associated ON

In the present study, daily oral administration of PE effectively reduced ON incidence to 31% as compared with 93% in control group, which was also evidenced by T1 weighed MR imaging. Neither animal death nor organ bleeding was documented in the PE-treated rabbits throughout the experimental period. This may suggest a potential long-term clinical application with required safety than available therapeutics combined with anticoagulant (Warfarin) tested experimentally [15]. Our results might also partially explain the fact that the remarkable difference in prevalence of ON found in SARS patients between North China (32.7%) [6] and South China (5–6%) [4,5] was associated with more frequent herbal prescription in South China than in North China [17].

The beneficial effect of PE on prevention of steroid-associated ON was demonstrated functionally and structurally, which shared the lights on the pathophysiological pathway in ON development, i.e., protecting structure–function of intra-osseous blood supply system from impairment by steroid-treatment. Two state-of-the-art imaging tools validated recently were applied in this study, which were validated in our previous one on the steroid-associated ON rabbit model [9]. Structurally, a high resolution MicroCT-based micro-angiography showed evidences of PE in maintaining vasculature with no blocked trunk vessels found in ON⁻ samples of the PE group compared to ON⁺ samples in the CON group. Functionally, a high-resolution contrast-enhanced Dynamic MRI for blood perfusion at the examined sites showed a significantly attenuated decrease in ‘Maximum Enhancement’, a function of local blood perfusion,

in the ON⁻ rabbits in the PE group than that of the ON⁺ rabbits in the CON group.

In addition, it is very interesting to find that numerous small disconnected vessels and disseminated leakage substance (Microfil) surrounded the blocked trunk vessels in CON group. It could be explained as abnormally permeable neovasculature formation induced by hypoxia due to local impaired blood supply system [41], which was suggested by both our published evidence (histogram of diameter of MicroCT-based intraosseous angiographic structural units) [9] and our un-published evidence (histology-based extensive edema lesion in marrow). Neither small disconnected vessels nor disseminated leakage substance found in PE group implied that local hypoxia was able to be prevented by PE. It really deserved further investigation on both ultrastructure of endothelium and signaling pathway of hypoxia-induced neovascularization and permeability in steroid-associated osteonecrosis [41].

A unique action mechanism associated with inhibition of both thrombosis and lipid deposition

Intravascular thrombosis-induced occlusion and extravascular lipid-deposit-induced compression have been regarded as two key pathogenic events of steroid-associated ON [2,3,8], which has been found in our recently established rabbit model synergistically induced by a combination of LPS and MPS [9].

In evaluation of pathogenic events, the present study used thrombus incidence as an indicator of intravascular thrombosis and marrow fat cell size as an indicator of extravascular lipid deposition, respectively. These two histopathological indicators showed that PE administration was able to inhibit both thrombosis and lipid deposition, which was evidenced by both significantly reduced thrombosis incidence and prominently smaller fat cell size in the PE group than that in the CON group.

In the present study for intravascular mechanistic investigation, both APTT (an indicator of coagulation) and tPA/PAI-I ratio (an indicator of hypofibrinolysis) were evaluated etiologically [10,11]. Haematological examination showed that PE could maintain balance between coagulation and fibrinolysis for inhibiting steroid-associated intravascular thrombophilia, which was evidenced by significantly attenuated decrease in both APTT and tPA/PAI-I ratio in the PE group as compared with that of the CON group.

In the present study for extravascular mechanistic investigation, two indicators were used etiologically. One is haematological LDL/HDL ratio, which reflects prominent lipid transport to the peripheral tissue (local bone tissue) [12]. The other is molecular PPAR γ 2mRNA expression of bone marrow cells, which is involved in adipogenesis [39]. Haematological data showed PE had a beneficial effect on reversing cholesterol transport, which was evidenced by significantly attenuated increasing in LDL/HDL ratio in the PE group as compared with that of the CON group. Molecular data indicated PE was able to inhibit excessive adipogenesis, which was evidenced by significantly attenuated increase in PPAR γ 2mRNA expression in the PE group as compared to that of the CON group.

Taken the above evaluations together, findings supported our hypothesis that PE exerted its beneficial effect on preventing development of steroid-associated ON with inhibition of both intravascular thrombosis and extravascular lipid deposition.

Limitation of the study

In the present study, PE reduced ON incidence to 31%, whereas a combination of anticoagulant plus a lipid-lowering agent reduced ON incidence to 5% in an early experimental study [15]. However, the combination therapeutics in Motomura et al.'s work started 1–2 weeks before inductive injection, and PE in our study started immediately after inductive injection. It is difficult to compare the prevention efficacy between those two experimental studies directly. Whether an introduction of a pretreatment with PE would help to reduce ON incidence, only further studies will tell. On the other hand, our histopathological results also showed PE did not decrease ON extension (numbers of ON lesion per affected rabbit) although it did decrease ON incidence significantly, which was consistent with Motomura G's experimental findings [15]. Based on Motomura G's outstanding discussion, it could be explained that there may be 'a threshold' beyond which ON development initiated, and PE may have modulated the threshold. Once the threshold was reached, PE had little effect on multi-focal nature of ON [15]. However, the future augmentation of prevention still depends on improved understandings of the 'threshold'.

In addition, the present study only involved single dose of PE established for prevention of osteoporosis [23], and dosing effects shall be further explored in the future to find out dose-dependent action manner for potential 'optimal' on reducing incidence of steroid-associated ON. On the other hand, there was only a 6-week duration for PE designed in our study. Prolonging observation duration by setting different time points should be valuable in the future study.

Furthermore, the PE used in the present study consisted of three phytoestrogenic compounds though with defined concentration [19,23]. It remains unclear how those phytoestrogenic compounds exerted their effects interactively on either intravascular event or extravascular events. It still deserves more specific experiments to investigate the interaction mechanism of PE compounds acting on the intravascular and extravascular events.

Conclusion and significance

The evidences obtained in the present study supported our hypothesis that a group of Epimedium-derived phytoestrogen fractions (PE) was able to exert beneficial effect on preventing development of steroid-associated osteonecrosis (ON) in rabbits with inhibition of both thrombosis and lipid deposition. A randomized, multi-center, controlled clinical trial is being investigated to evaluate the potential application of the PE to prevent steroid-associated ON in patients with high risk.

References

- [1] Assouline-Dayan Y, Chang C, Greenspan A, et al. Pathogenesis and natural history of osteonecrosis. *Semin Arthritis Rheum* 2002;32:94–124.
- [2] Lieberman JR, Berry DJ, Mont MA, et al. Osteonecrosis of the hip: management in the 21st century. *Instr Course Lect* 2003;52:337–55.
- [3] Wang GJ, Cui Q, Balian G. The pathogenesis and prevention of steroid-induced osteonecrosis. *Clin Orthop Relat Res* 2000;295–310.
- [4] Griffith JF, Antonio GE, Kumta SM, et al. Osteonecrosis of hip and knee in patients with severe acute respiratory syndrome treated with steroids. *Radiology* 2005;235:168–75.
- [5] Shen J, Liang BL, Zeng QS, et al. Report on the investigation of lower extremity osteonecrosis with magnetic resonance imaging in recovered severe acute respiratory syndrome in Guangzhou. *Zhonghua Yixue Zazhi* 2004;84:1814–7.
- [6] Li ZR, Sun W, Qu H, et al. Clinical research of correlation between osteonecrosis and steroid. *Zhonghua Waikexue Zazhi* 2005;43:1048–53.
- [7] Saito S, Saito M, Nishina T, et al. Long-term results of total hip arthroplasty for osteonecrosis of the femoral head. A comparison with osteoarthritis. *Clin Orthop Relat Res* 1989;244:198–207.
- [8] Aaron RK. Osteonecrosis: etiology, pathophysiology and diagnosis. In: Callaghan JJ, et al, editor. *The adult hip*. Philadelphia: Lippincott-Raven; 1998. p. 457.
- [9] Qin Ling, Zhang G, Sheng H, et al. Multiple imaging modalities in evaluation of experimental osteonecrosis induced by a combination of lippolysaccharide and methylprednisolone. *Bone* 2006;39:863–71.
- [10] Glueck CJ, Freiberg RA, Fontaine RN, et al. Hypofibrinolysis, thrombophilia, osteonecrosis. *Clin Orthop Relat Res* 2001;386:19–33.
- [11] Glueck CJ, Freiberg RA, Wang P. Role of thrombosis in osteonecrosis. *Curr Hematol Rep* 2003;2:417–22.
- [12] Miyanishi K, Yamamoto T, Irisa T, et al. A high low-density lipoprotein cholesterol to high-density lipoprotein cholesterol ratio as a potential risk factor for corticosteroid-induced osteonecrosis in rabbits. *Rheumatology (Oxford)* 2001;40:196–201.
- [13] Li X, Jin L, Cui Q, et al. Steroid effects on osteogenesis through mesenchymal cell gene expression. *Osteoporos Int* 2005;16:101–8.
- [14] Irisa T, Yamamoto T, Miyanishi K, et al. Osteonecrosis induced by a single administration of low-dose lipopolysaccharide in rabbits. *Bone* 2001;28:641–9.
- [15] Motomura G, Yamamoto T, Miyanishi K, et al. Combined effects of an anticoagulant and a lipid-lowering agent on the prevention of steroid-induced osteonecrosis in rabbits. *Arthritis Rheum* 2004;50:3387–91.
- [16] So LK, Lau AC, Yam LY, et al. Development of a standard treatment protocol for severe acute respiratory syndrome. *Lancet* 2003;361:1615–7.
- [17] Lau TF, Leung PC, Wong EL, et al. Using herbal medicine as a means of prevention experience during the SARS crisis. *Am J Chin Med* 2005;33:345–56.
- [18] Liu X, Zhang M, He L, et al. Chinese herbs combined with Western medicine for severe acute respiratory syndrome (SARS). *Cochrane Database Syst Rev* 2006;1:CD004882.
- [19] Qin L, Zhang G, Shi YY, et al. Prevention and treatment of osteoporosis with traditional herbal medicine. In: Deng HW, et al, editor. *Current topics of osteoporosis*. World Scientific Publisher; 2005. p. 513–31.
- [20] Lee SH, Jung BH, Kim SY, et al. Determination of phytoestrogens in traditional medicinal herbs using gas chromatography-mass spectrometry. *J Nutr Biochem* 2004;15:452–60.
- [21] Meng FH, Li YB, Xiong ZL, et al. Osteoblastic proliferative activity of *Epimedium brevicornum Maxim*. *Phytomedicine* 2005;12:189–93.
- [22] Qin L, Zhang G, Hung WY, et al. Phytoestrogen-rich herb formula "XLGB" prevents OVX-induced deterioration of musculoskeletal tissues at the hip in old rats. *J Bone Miner Metab* 2005;23S:55–61.
- [23] Zhang G, Qin L, Hung WY, et al. Flavonoids derived from herbal *Epimedium brevicornum Maxim* prevent OVX-induced osteoporosis in rats independent of its enhancement in intestinal calcium absorption. *Bone* 2006;38:818–25.
- [24] Clifton-Bligh PB, Baber RJ, Fulcher GR, et al. The effect of isoflavones extracted from red clover (Rimostil) on lipid and bone metabolism. *Menopause* 2001;8:259–65.

- [25] Lamon-Fava S. Genistein activates apolipoprotein A-I gene expression in the human hepatoma cell line Hep G2. *J Nutr* 2000;130:2489–92.
- [26] Anderson JW, Johnstone BM, Cook-Newell ME. Meta-analysis of the effects of soy protein intake on serum lipids. *N Engl J Med* 1995;333:276–82.
- [27] Dang ZC, van Bezooijen RL, Karperien M, et al. Exposure of KS483 cells to estrogen enhances osteogenesis and inhibits adipogenesis. *J Bone Miner Res* 2002;17:394–405.
- [28] Dang ZC, Audinot V, Papapoulos SE, et al. Peroxisome proliferator-activated receptor gamma (PPARgamma) as a molecular target for the soy phytoestrogen genistein. *J Biol Chem* 2003;278:962–7.
- [29] Dang Z, Lowik CW. The balance between concurrent activation of ERs and PPARs determines daidzein-induced osteogenesis and adipogenesis. *J Bone Miner Res* 2004;19:361–853.
- [30] Cooke PS, Naaz A. Effects of estrogens and the phytoestrogen genistein on adipogenesis and lipogenesis in males and females. *Birth Defects Res, A Clin Mol Teratol* 2005;73:472–3.
- [31] Wang W, Zhu GJ, Zu SY. Effects of 17 β estradiol and phytoestrogen α -zearalanolone on coagulation and fibrinolysis in rats. *Chin J Arterioscler* 2004;12:139–42.
- [32] Choo MK, Park EK, Yoon HK, et al. Antithrombotic and antiallergic activities of daidzein, a metabolite of puerarin and daidzin produced by human intestinal microflora. *Biol Pharm Bull* 2002;25:1328–32.
- [33] Beresford JN, Owen ME. Marrow stromal cell culture. Cambridge Univ. Press; 1998.
- [34] Chen WT, Shih TT, Chen RC, et al. Blood perfusion of vertebral lesions evaluated with gadolinium-enhanced dynamic MRI: in comparison with compression fracture and metastasis. *J Magn Reson Imaging* 2002;15:308–14.
- [35] Duvall CL, Robert Taylor W, Weiss D, et al. Quantitative microcomputed tomography analysis of collateral vessel development after ischemic injury. *Am J Physiol: Heart Circ Physiol* 2004;287:H302–10.
- [36] Qin L, MakF AT, Cheng CW, et al. Histomorphological study on pattern of fluid movement in cortical bone in goats. *Anat Rec* 1999;255:380–7.
- [37] Yamamoto T, Irisa T, Sugioka Y, et al. Effects of pulse methylprednisolone on bone and marrow tissues: corticosteroid-induced osteonecrosis in rabbits. *Arthritis Rheum* 1997;40:2055–64.
- [38] Yamamoto T, Hirano K, Tsutsui H, et al. Corticosteroid enhances the experimental induction of osteonecrosis in rabbits with Shwartzman reaction. *Clin Orthop Relat Res* 1995;316:235–43.
- [39] Lazar MA. PPAR gamma, 10 years later. *Biochimie* 2005;87:9–13.
- [40] Ji RR, Li FY, Zhang XJ. Effect of flavone glycosides of *Epimedium koreanum* on murine fibrinolytic system and apopleptic mortality. *Zhongguo Zhong-Xiyi Jiehe Zazhi* 2005;25:525–30.
- [41] Weis SM, Cheresh DA. Pathophysiological consequences of VEGF-induced vascular permeability. *Nature* 2005;437:497–504.